Electronic structure of the Chevrel-phase compounds $Sn_xMo_6Se_{7.5}$: Photoemission spectroscopy and band-structure calculations

K. Kobayashi*
Department of Physics, University of Tokyo, Hongo 7-3-1, Bunkyo-ku, Tokyo 113-0033, Japan

A. Fujimori
Department of Physics and Department of Complexity Science and Engineering, University of Tokyo, Bunkyo-ku, Tokyo 113-0033, Japan

T. Ohtani
Laboratory for Solid State Chemistry, Okayama University of Science, Ridai-cho 1-1, Okayama 700-0005, Japan

I. Dasgupta,† O. Jepsen, and O. K. Andersen
Max-Planck-Institut für Festkörperforschung, Postfach 800665, D-70506, Stuttgart, Germany
(Received 15 September 2000; published 26 April 2001)

We have studied the electronic structure of two Chevrel-phase compounds, $Mo_6Se_{7.5}$ and $Sn_{1.2}Mo_6Se_{7.5}$, by combining photoemission spectroscopy and band-structure calculations. Core-level spectra taken with x-ray photoemission spectroscopy show systematic core-level shifts, which do not obey a simple rigid-band model. The inverse photoemission spectra imply the existence of an energy gap located ~1 eV above the Fermi level, which is a characteristic feature of the electronic structure of the Chevrel compounds. Quantitative comparisons between the photoemission spectra and the band-structure calculations have been made. While good agreement between theory and experiment in a wide energy range was obtained as already reported in previous studies, we found that the high density of states near the Fermi level predicted theoretically due to the Van Hove singularity is considerably reduced in the experimental spectra taken with higher energy resolution than in previous reports. Possible explanations for this observation are proposed.

DOI: 10.1103/PhysRevB.63.195109 PACS number(s): 79.60.−i, 74.70.Ad, 71.20.−b, 74.25.Jb

I. INTRODUCTION

The Chevrel-phase compounds, which were extensively studied in the 1970s as one of the largest families of superconductors,[1–3] have recently attracted renewed interest as candidates for thermoelectric materials.[4,5] Their general formula is $A_xMo_6X_8$, where X is a chalcogen atom, namely, S, Se, or Te and A is an alkali metal, alkaline earth, simple metal, transition metal, noble metal, or rare earth.[2] Dozens of compounds with this formula are known, a large portion of which show superconductivity. Crystallographically, they have a rather remarkable structure consisting of Mo_6X_8 clusters. In this sense, the Chevrel system is a forerunner of cluster-based superconductors like the fullerenes. Such materials tend to have rather exotic electronic structures, which gives us a unique opportunity to search for compounds with unusual properties.

A number of theoretical band-structure calculations have been reported for the Chevrel-phase compounds.[6–10] Two characteristic features should be remarked. The first is the high density of states (DOS) near the Fermi level (E_F) mainly due to flatbands of Mo $4d$ character, which would favor a high superconducting transition temperature according to standard BCS theory. In fact, the Fermi level is located close to a Van Hove singularity (VHS).[8] In addition, the flatbands mean a low Fermi velocity, which leads to a short coherence length and hence a high critical magnetic field (H_{C2}).[3] Second, there exists an energy-gap-like structure about 1 eV above E_F. This arises from a splitting between the bonding and antibonding states of the Mo $4d$ manifold and its position relative to E_F depends on the number of electrons in the cluster. It is this feature as well as the cluster-based crystal structure that gives some researchers the hope that thermoelectric materials may exist among the Chevrel-phase compounds.[4,5]

Experimentally, photoemission spectroscopy (PES) is one of the most useful methods to investigate the electronic structures, and it has already been applied to this system several times. Following the early work by Ihara and Kimura,[11] many studies have been reported including x-ray photoemission spectroscopy (XPS), ultraviolet photoemission spectroscopy (UPS),[12–17] and x-ray emission spectroscopy.[12] Although the measured valence-band spectra were compared with band-structure calculations and good agreement was obtained between experiment and theory,[12,13] experiments have not been performed using high enough resolution to access the electronic structure near E_F. Information about the unoccupied states that could be obtained by inverse photoemission spectroscopy (IPES) is also lacking.

In this paper, we report on a study of the electronic structure of two Chevrel-phase compounds $Mo_6Se_{7.5}$ and $Sn_{1.2}Mo_6Se_{7.5}$, combining the results of PES, IPES, and band-structure calculations. First, the experimental results for the core-level, valence-band, and conduction-band spectra will be shown. The valence-band spectra were taken with much higher resolution than in previous reports. Second, after the results of the band-structure calculations for Mo_6Se_8 and $SnMo_6Se_8$ are reported, a quantitative comparison between the experimental PES and IPES spectra and the theoretical spectra derived from the band-structure calculations

 ©2001 The American Physical Society

will be made. We finally discuss to what extent the theory explains the experimental results.

II. EXPERIMENT

A. Sample preparation

Polycrystalline samples of $Mo_6Se_{7.5}$ and $Sn_{1.2}Mo_6Se_{7.5}$ were prepared as follows. For $Mo_6Se_{7.5}$, a mixture of Mo and Se with the desired ratio was sealed in an evacuated silica tube, and was then heated from 200 °C to 900 °C at a rate of 100 °C/h, followed by annealing at 900 °C for 12 h. The product was ground and pressed into a pellet, and was then annealed at 1200 °C for three days. For $Sn_{1.2}Mo_6Se_{7.5}$, a mixture of the desired ratio of Sn, Mo and Se powders was heated in an evacuated silica tube at 200 °C for 12 h and at 250 °C for 12 h, and was then heated up to 800 °C at a rate of 100 °C/h, followed by annealing at 800 °C for 24 h. The product was pressed into a pellet and was annealed again at 1000 °C for a week. X-ray diffraction patterns of both samples were successfully indexed on the basis of the Chevrel structure. The hexagonal lattice parameters were determined to be $a=9.568$ Å and 9.521 Å and $c=11.180$ Å and 11.838 Å for $Mo_6Se_{7.5}$ and $Sn_{1.2}Mo_6Se_{7.5}$, respectively. The $Sn_xMo_6Se_8$ phases were stabilized when the atomic ratio between Mo and Se was slightly nonstoichiometric. While the x-ray diffraction does not show any extra phase caused by the nonstoichiometry, it is not known whether Se deficiency or excess Mo is responsible for this nonstoichiometry.[18] Judging from the results for the sulfide Chevrel-phase compounds,[19] however, the former is more likely rather than the latter. Transitions to superconducting states were found to occur at 5–8 K for $Mo_6Se_{7.5}$ and 2–8 K for $Sn_{1.2}Mo_6Se_{7.5}$, consistent with previous reports.

B. Photoemission measurements

The XPS measurements were done using the Mg $K\alpha$ line ($h\nu=1253.6$ eV) and photoelectrons were collected using a PHI double-pass cylindrical-mirror analyzer. The UPS measurements were made using the He I and He II resonance lines ($h\nu=21.2$ eV and 40.8 eV, respectively) and a VSW hemispherical analyzer. The IPES or Bremsstrahlung-isochromat spectroscopy (BIS) measurements were performed by detecting photons of $h\nu=1486.6$ eV using a quartz monochromator. The XPS and BIS measurements were made at liquid-nitrogen temperature, and the UPS measurements at ~28 K. We did the energy calibration and the estimation of the instrumental resolution by using Au evaporated on the surface of the samples after each measurement. They were performed for XPS by defining Au $4f_{7/2}=84.0$ eV, and for UPS and BIS by measuring the Fermi edge. The total resolution was ~1 eV, ~35 meV, ~80 meV, and ~1 eV for XPS, He I UPS, He II UPS, and BIS, respectively.

The samples were scraped *in situ* with a diamond file for every measurement. During the XPS measurements, the intensity of the O 1*s* core-level signal, which indicates contaminations on the sample surfaces, did not increase for several hours, once it had been almost removed. Therefore, the measurements of XPS and BIS were undertaken by scraping the samples every several hours. However, scraping was done more frequently for the UPS measurements because UPS is more surface sensitive than XPS and BIS.

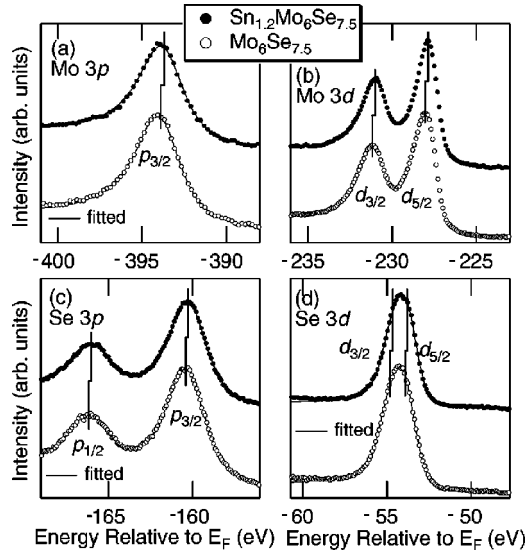

FIG. 1. Mo 3*p* (a), Mo 3*d* (b), Se 3*p* (c), and Se 3*d* (d) core-level spectra of $Sn_{1.2}Mo_6Se_{7.5}$ and $Mo_6Se_{7.5}$ indicated by closed and open circles, respectively. In (a), (c), and (d), the results of the line-shape fitting are also shown by solid curves with vertical bars indicating the peak positions obtained through the line-shape analysis. Only in (b) are the positions of the intensity maxima indicated with vertical bars since the Mo 3*d* spectra contain signals from the Se 3*s* core level. The peak positions obtained are listed in Table I below.

III. EXPERIMENTAL RESULTS

A. Core-level spectra

Figures 1(a), 1(b), 1(c), and 1(d) show the Mo 3*p*, Mo 3*d*, Se 3*p*, and Se 3*d* core-level spectra of $Mo_6Se_{7.5}$ and $Sn_{1.2}Mo_6Se_{7.5}$ obtained by XPS, respectively. The horizontal axis (E) measures the energy relative to E_F and the binding energy (E_B) is given by $-E$. Two observations are worth mentioning. First, systematic core-level shifts occur in going from $Mo_6Se_{7.5}$ to $Sn_{1.2}Mo_6Se_{7.5}$. Second, the line shape of the Mo core level looks more asymmetric with a longer tail toward higher binding energy than that of the Se core level. This is a feature common to both compounds.

To be more quantitative on those points, we made a line-shape analysis by means of least-squares fitting. It is assumed that each core-level peak has Mahan's asymmetric line-shape reflecting the effect of core-hole screening by conduction electrons in metals.[20] The degree of asymmetry is characterized by the singularity index α given by

$$\alpha=2\sum_l (2l+1)\left(\frac{\delta_l}{\pi}\right)^2=\sum_l \frac{q_l^2}{2(2l+1)}, \qquad (1)$$

where q_l is the charge of the conduction electrons with angular momentum l which screens the core hole and δ_l is the phase shift, satisfying Friedel's sum rule $\Sigma_l q_l=1$. The line

TABLE I. Core-level peak position E and singularity index α obtained by the line-shape analysis. For the Mo $3d$ core level only, the peak positions determined by their intensity maxima are listed. ΔE denotes the spin-orbit splitting between $3p_{3/2}$ and $3p_{1/2}$ or between $3d_{5/2}$ and $3d_{3/2}$.

	$Mo_6Se_{7.5}$			$Sn_{1.2}Mo_6Se_{7.5}$		
Core level	E (eV)	ΔE (eV)	α	E (eV)	ΔE (eV)	α
Mo $3p_{3/2}$	−393.87	17.52	~0.18	−393.67	17.52	~0.18
Mo $3d_{5/2}$	−228.03	3.13		−227.88	3.14	
Se $3p_{3/2}$	−160.38	5.77	<0.02	−160.27	5.77	<0.01
Se $3d_{5/2}$	−53.91	0.91	~0.05	−53.78	0.88	~0.07

shape is convoluted with a Gaussian and a Lorentzian function which represent the instrumental resolution and the core-hole lifetime broadening, respectively. An integral background[20] is also assumed. The line-shape analysis was successfully made except for the Mo $3d$ core-level spectra which contain a weak Se $3s$ core-level peak at $E\sim -229$ eV. The results are shown for the Mo $3p$, Se $3p$, and Se $3d$ core-level spectra of both compounds in Figs. 1(a), 1(c), and 1(d) by solid curves. The fit parameters are shown in Table I.

First, it is found from Table I that the singularity indices of the Mo core levels are larger than those of the Se core levels, in qualitative agreement with the results for the sulfide Chevrel-phase compound.[13] This observation indicates that the contribution from the Mo $4d$ electrons is dominant at E_F rather than that from Se $4p$, which is qualitatively consistent with the band-structure calculations. Second, we also found that each core level in $Mo_6Se_{7.5}$ is located at a binding energy that is 0.1–0.2 eV higher than that in $Sn_{1.2}Mo_6Se_{7.5}$. As for the trend of the core-level shifts, it has been reported that the shifts have weak linear correlation with the intercluster Mo-Mo distance and the rhombohedral lattice parameter of Chevrel systems judging from the core-level and Mo $1s$ absorption spectra of various $A_xMo_6X_8$ compounds (A=Pb, Ni, Cu, and so on and X=S, Se, and Te).[16] Our results follow the same trend in that E_B increases as the Mo-Mo distance increases. Since the total number of electrons in the cluster increases when Sn is added to $Mo_6Se_{7.5}$, the rigid-band model predicts that each core-level binding energy should increase in going from $Mo_6Se_{7.5}$ to $Sn_{1.2}Mo_6Se_{7.5}$. The observed core-level shifts are therefore opposite to those expected from the rigid-band model, assuming that Sn is an electron donor and that the Fermi level would be raised by Sn doping. Thus, our results imply that the valence-band structure itself changes and the system behaves unlike a rigid-band model when Sn is added interstitially to $Mo_6Se_{7.5}$.

B. Valence-band photoemission spectra

The valence-band XPS and UPS spectra of $Mo_6Se_{7.5}$ and $Sn_{1.2}Mo_6Se_{7.5}$ in the entire valence band and in the vicinity of E_F are shown in Figs. 2(a) and 2(b), respectively. They were normalized to the area of the whole valence band, which spreads between $E\sim -8$ eV and 0 eV after backgrounds of integral type[20] and Henrich type[21] had been subtracted for the XPS and UPS spectra, respectively.

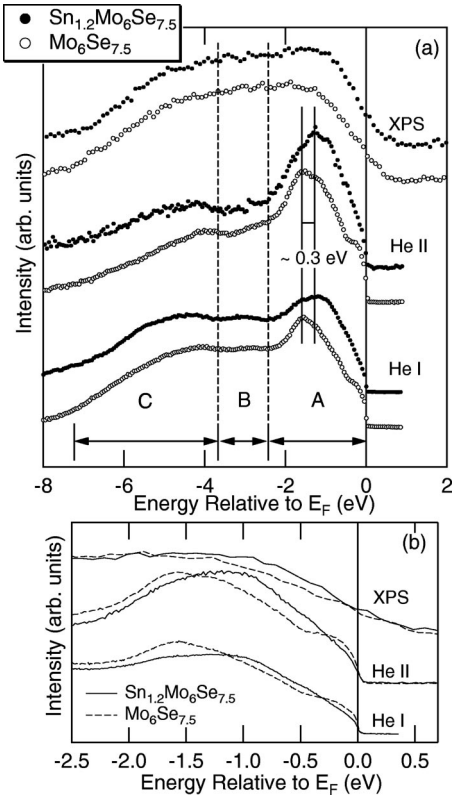

FIG. 2. Valence-band photoemission spectra of $Mo_6Se_{7.5}$ and $Sn_{1.2}Mo_6Se_{7.5}$ in the entire valence band (a) and in the vicinity of E_F (b). The photon energies used for the measurements are $h\nu$ =21.2 eV (He I UPS), 40.8 eV (He II UPS), and 1253.6 eV (XPS). All the spectra were normalized to the area between $E=-8$ eV and 0 eV after backgrounds of integral type and of Henrich type were subtracted for the XPS and UPS spectra, respectively.

Roughly speaking, three structures are identified in the spectra of both compounds. For the moment, these structures are referred to as A (from 0 to ~ -2 eV), B(~ -3 eV), and C (from ~ -4 to ~ -7 eV) as indicated in the figure. Because the Sn $5s$ core level is observed at $E\sim -14$ eV, we have to take into account only Mo $4d$ and Se $4p$. The contribution of Mo $5s$ and Sn $5sp$ to the valence-band spectra is negligible because of their small numbers of electrons in these compounds and their relatively small cross sections.[22] Based on the fact that the relative cross section of Se $4p$ to Mo $4d$ is largest at $h\nu$=1253.6 eV (XPS) and smallest at 40.8 eV (He II UPS), we can consider A to be of mainly Mo $4d$ character, showing up as a distinct peak in the He I and He II UPS spectra. In a similar way, structures B and C are attributed to Se $4p$ character because they appear as strong broad features in XPS. In the XPS spectra, it is hard to discriminate between B and C because of the low energy resolution. The above assignment is qualitatively consistent with the band-structure calculations (see Fig. 4 below): Mo $4d$ character is dominant in the rather narrow energy range from $E=0$ to ~ -2 eV and Se $4p$ character appears as a broad band from $E\sim -3$ to ~ -7 eV. Quantitative comparison will be made below.

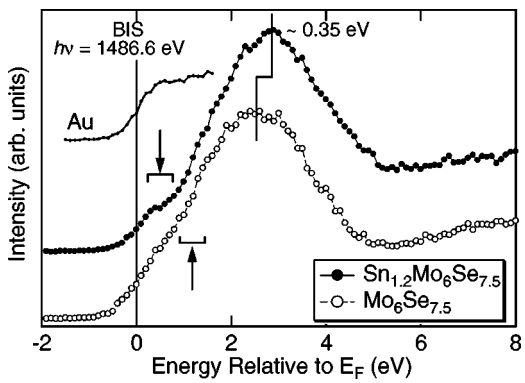

FIG. 3. BIS spectra of $Sn_{1.2}Mo_6Se_{7.5}$ and $Mo_6Se_{7.5}$. The arrows indicate the shoulder around 1 eV above E_F. At the top, the spectrum of gold is also plotted.

The intensity between $E=-0.3$ and -1.2 eV of $Sn_{1.2}Mo_6Se_{7.5}$ is higher than that of $Mo_6Se_{7.5}$, which holds true for all three spectra as seen in Fig. 2(b). Here, it may be tempting to consider that the Mo $4d$ band of $Mo_6Se_{7.5}$ is shifted by $\sim$0.3 eV to higher binding energy compared with that of $Sn_{1.2}Mo_6Se_{7.5}$, corresponding to the core-level shift. We should, however, emphasize again that the rigid-band model predicts the opposite. Indeed, the line shape around E_F is qualitatively different for the two compounds, which clearly means that a simple rigid-band model is not applicable to the Chevrel system and that the insertion of Sn atoms between the clusters certainly changes the electronic structure around E_F. Alternatively, the shift can be partly attributed to the narrowing of the Mo $4d$ band due to the increase in the distance between the Mo_6Se_8 clusters. Generally, when the X atom in the Mo_6X_8 cluster goes from S to Se, the lattice parameters increase due to the larger atomic radius of Se. In a similar way, by inserting large atoms such as Sn and Pb, the distance between the clusters increases.[3] This results in the decrease of the Mo $4d$ bandwidth, and in turn lowers the position of E_F relative to the other core and valence levels because the Fermi level is located close to the top of the Mo $4d$ band in the bonding states. Actually, a slight decrease of the Mo $4d$ band width from Mo_6Se_8 to $SnMo_6Se_8$ is also predicted in the band-structure calculations as reported below.

C. BIS spectra

The BIS spectra of $Sn_{1.2}Mo_6Se_{7.5}$ and $Mo_6Se_{7.5}$ are shown in Fig. 3 with closed and open circles, respectively. The BIS spectrum of Au near the Fermi level is also shown at the top of the figure for the sake of comparison. The main peak at $E\sim2$ eV is readily assigned to Mo $4d$ character, namely, the antibonding states of the Mo $4d$ band, because Mo $4d$ has a high density of unoccupied states and its cross section is larger than the other components such as Se $4p$. The broad structure at $E\gtrsim6$ eV is of Mo $4p$ character. As marked in Fig. 3, the main peak position of $Sn_{1.2}Mo_6Se_{7.5}$ is shifted to higher energy relative to that of $Mo_6Se_{7.5}$ by $\sim$0.35 eV. This shift and its direction are consistent with the PES results, and is explained in the same way as above: in going from $Mo_6Se_{7.5}$ to $Sn_{1.2}Mo_6Se_{7.5}$, the narrowing of the Mo $4d$ bands occurs not only in the bonding state but also in the antibonding state and the position of E_F is lowered relative to the core levels. On the other hand, the centroid of the band in both states should be unaffected by the narrowing in the first approximation, causing the Mo $4d$ peak in the unoccupied state to be shifted away from E_F in the $Sn_{1.2}Mo_6Se_{7.5}$ spectra.

Now, a characteristic feature in Fig. 3 is the existence of a shoulder at $E\sim0.5$ eV in the $Sn_{1.2}Mo_6Se_{7.5}$ spectrum as marked by an arrow in the figure. This shoulder implies the existence of a dip in the unoccupied DOS. Though not so obvious as in the $Sn_{1.2}Mo_6Se_{7.5}$ spectrum, there is a similar shoulder at $E\sim1$ eV in the $Mo_6Se_{7.5}$ spectrum. As mentioned above, the band-structure calculations for many Chevrel-phase compounds[6–10] have predicted the existence of an energy gap around 1 eV above E_F. The observed shoulder is consistent with this considering the $\sim$1 eV energy resolution of the BIS measurements [see Fig. 5(a) below]. To the best of our knowledge, the above observation is the first experimental indication of the existence of the gap above E_F in Chevrel-phase compounds.

IV. BAND-STRUCTURE CALCULATIONS

In order to interpret the experimental results from a theoretical viewpoint, we have performed band-structure calculations for both compounds. The band structure was calculated self-consistently using the local density-functional approximation (LDA) and the scalar relativistic linear muffin-tin orbital method (LMTO) in the atomic sphere approximation (ASA) including the combined correction (CC).[23–25]

In the ASA+CC, the one-electron potential entering the Schrödinger equation is a superposition of overlapping spherical potential wells with a position R and radii s_R, plus a kinetic energy error proportional to the fourth power of the relative overlap of the spheres. The radii of the overlapping muffin-tin spheres are determined by the conditions that the overlapping muffin-tin potential be the best possible approximation to the full potential, and that the error due to sphere overlap be acceptable. For the Chevrel phases with open structure, these conditions cannot be achieved with only atom centered spheres so several interstitial (empty) spheres were included to achieve good sphere packing and an overall good representation of the potential. The radii of the atomic and interstitial spheres as well as the position of the interstitial spheres were calculated by using an automatic procedure developed by Krier *et al.*[26] In the present calculation we allowed an overlap of 16% between atom centered spheres, 18% between atom centered and interstitial spheres, and 20% between interstitial spheres.

The basis set for both compounds consisted of Mo $5s$, $5p$, $4d$, Se $4p$, and the interstitial s LMTO's. In addition for $SnMo_6Se_8$ we included Sn $5s$,$5p$ LMTO's. Se s, d, Sn d, and interstitial p-d were downfolded.[27] This treatment not only reduced the size of the secular matrix but also avoided distortions of the phase shift of the high partial waves. Such distortions, or even ghost bands, may occur with the conventional LMTO method. All k-space integrations were per-

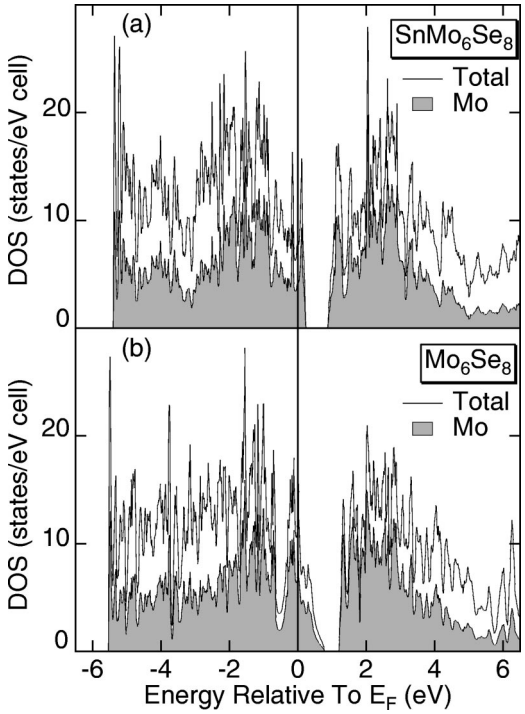

FIG. 4. Calculated DOS of (a) $SnMo_6Se_8$ and (b) Mo_6Se_8 with the total DOS and Mo 4d partial DOS shown by the solid line and the shaded area, respectively.

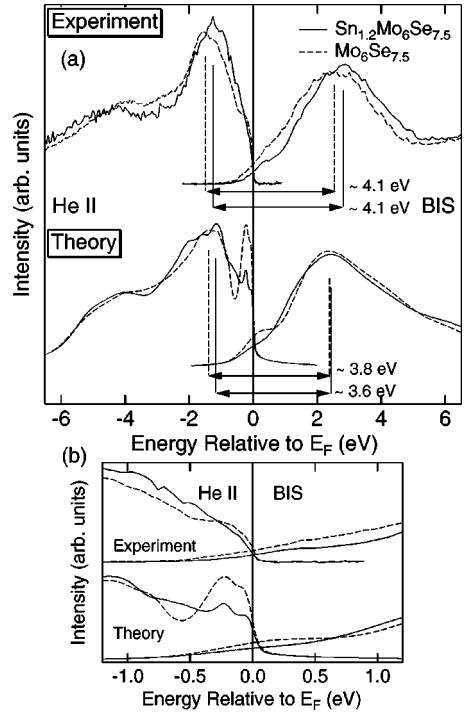

FIG. 5. (a) Comparison between theory and experiment for the He II and BIS spectra of $Sn_{1.2}Mo_6Se_{7.5}$ with solid curves and $Mo_6Se_{7.5}$ with dashed curves in a wide energy range. The solid and dashed vertical bars indicate the positions of the intensity maxima of the main structures of the $Sn_{1.2}Mo_6Se_{7.5}$ and $Mo_6Se_{7.5}$ spectra, respectively. The energy splitting between the bonding and antibonding states of the Mo 4d band is also shown. (b) The enlarged plots of (a) in the vicinity of E_F.

formed by the tetrahedron method[28] using 254 irreducible k points within the Brillouin zone.

The calculated densities of states are shown in Figs. 4(a) and 4(b) for $SnMo_6Se_8$ and Mo_6Se_8, respectively, and they are consistent with previous reports on other Chevrel-phase compounds.[6–10] For example, Mo_6Se_8 and $SnMo_6Se_8$ are calculated to have four and two holes between E_F and the top of the valence band, respectively, as was previously reported. The DOS at E_F is very high and situated near the VHS, which explains the asymmetric line shape of the Mo core-level spectra. The width of the Mo 4d band in the bonding states decreases from 6.4 eV to 5.7 eV in going from Mo_6Se_8 to $SnMo_6Se_8$, which may be partly responsible for the aforementioned non-rigid-band-like behavior. It should be noted here that the role of the insertion of Sn atoms between the clusters is to change not only the number of electrons but also the cluster-cluster interactions.

V. COMPARISON BETWEEN THEORY AND EXPERIMENT

In this section, we will make a quantitative comparison between the photoemission spectra and theoretical spectra derived from the band-structure calculations. First, it is necessary to redefine the Fermi level of the calculation, because due to the Se deficiency the Fermi level of $Sn_{1.2}Mo_6Se_{7.5}$ ($Mo_6Se_{7.5}$) is apparently higher than that of $SnMo_6Se_8$(Mo_6Se_8) by 1.4 (1.0) electrons on the assumption that each Se vacancy gives two electrons to the valence band. The shift corresponding to this in the band-structure calculation is 0.072 eV and 0.085 eV for $Sn_{1.2}Mo_6Se_{7.5}$ and $Mo_6Se_{7.5}$, respectively. To derive the theoretical photoemission spectra from the results shown in Fig. 4 we took into account the contribution of Mo 4d and Se 4p only. The partial DOS of each component has been weighted by the corresponding photoionization cross section at each photon energy, and this weighted DOS has been broadened by convoluting with a Gaussian and a Lorentzian which represent the instrumental resolution and the lifetime broadening, respectively. We have assumed that the lifetime width is linear in energy E measured from E_F, i.e., the full width at half maximum $w=\alpha|E-E_F|$. The coefficient α, which phenomenologically represents the size of the lifetime of the photohole with increasing binding energy, is a parameter that is determined so that the measured spectra are well reproduced. For both compounds we have taken $\alpha=0.24$ and 0.40 for the photoemission and inverse-photoemission spectra, respectively. The spectra have been normalized to their total area.

As shown in Fig. 5(a), the agreement in a wide energy range between theory and experiment is quite satisfactory, as has already been reported.[12,13] The main features observed around $E=2$–3 eV, $-(1$–$2)$ eV, and $-(3$–$6)$ eV in the BIS and PES spectra are well reproduced in the theoretical simulation. As shown in the figure, the energy difference between the main peak in the He II spectrum and that in the BIS spectrum equals ~4.1 eV for both compounds, while the counterpart in the theory is ~3.8 eV for $Mo_6Se_{7.5}$ and ~3.6

eV for $Sn_{1.2}Mo_6Se_{7.5}$. Although the theoretical values are slightly smaller than the experimental ones, the values of the energy splittings, which directly reflect the electronic structure of the Mo_6Se_8 cluster, fall in the same range for both theory and experiment. In the theoretical studies, it is known that a molecular-cluster approach is a good first approximation,[9] due to the localized nature of the Mo $4d$ electrons within the cluster.

In spite of that agreement, however, there exists a large discrepancy just around E_F between the experimental and theoretical He II spectra as shown in Fig. 5(b): while the intensity of the $Mo_6Se_{7.5}$ spectrum is larger than that of the $Sn_{1.2}Mo_6Se_{7.5}$ spectrum, which qualitatively holds true in theory and experiment, the absolute intensity is not reproduced at all. Indeed, the sharp peak in the theoretical spectrum originating from the VHS completely disappears in the experimental spectrum. Although the energy resolution is not high enough to check this point for the BIS spectra, one can see a similar tendency there too. We believe that the disappearance of the VHS is intrinsic judging from the overall good agreement between theory and experiment in the wide energy range. Actually, there are several effects that have been neglected in the band-structure calculations. The remarkable reduction of the PES intensity near E_F indicates that such an effect plays a significant role in the spectra on the low energy scale. Because the total spectral weight should be conserved if integrated to a sufficiently high energy, the significant weight near E_F that is theoretically predicted is supposed to be transferred to the region away from E_F (at least 1–2 eV from E_F) in the experimental spectra. A similar discrepancy between theory and experiment exists in the photoemission spectra of another cluster-based superconductor, K_3C_{60}.[29]

Several candidates that can cause the above phenomenon may be listed. First, disorder due to the nonstoichiometry: The Se deficiency (and the excess of Sn for $Sn_{1.2}Mo_6Se_{7.5}$) may create a random potential that reduces the coherence of the electrons, leading to the decrease of the spectral intensity near E_F. It has been reported that static disorder causes such an effect in the PES spectrum of $TaSe_2$.[30] A PES study for more stoichiometric single crystals of Chevrel-phase compounds will clarify this point. Second, we may consider electron-phonon interactions. It has been reported that the electron-phonon coupling constant (λ) in a Chevrel-phase compound is as large as ~ 1 (Ref. 3), a value that may reduce the spectral intensity to almost half of the theoretical value.[31] The same explanation has been made for K_3C_{60}.[32] The typical energy of phonons in the Chevrel-phase compounds is, however, only ~ 10 meV (Ref. 3), which cannot cause a transfer of spectral weight of the order of $\gtrsim 1$ eV. The third candidate is the electron-electron interaction, which is presumably significant in the Mo_6Se_8 clusters containing localized $4d$ electrons. In $3d$-transition-metal oxides with strong electron correlation, for example, it has been reported that the large spectral weight around E_F is transferred to higher binding energy farther from E_F as an ''incoherent'' part.[33,34] While not only one but a combination of these three effects may thoroughly explain the discrepancy between theory and experiment, the electron-electron interaction is the most likely to be responsible among them, because a transfer of spectral weight of the order of $\gtrsim 1$ eV can be explained only by taking this interaction into account. In fact, the significance of electron correlation effects in the Mo $4d$ band in the Chevrel cluster were previously pointed out by Brusetti *et al.*[35] Finally, it should be remarked that the vanishing of the high DOS due to the VHS is not peculiar to this system but has been observed in several superconductors such as the borocarbides and the $A15$ compounds.[36] The reason for this universal observation remains to be clarified in the future.

VI. CONCLUSION

We have studied the electronic structure of two Chevrel-phase compounds, $Mo_6Se_{7.5}$ and $Sn_{1.2}Mo_6Se_{7.5}$, using PES experiment and band-structure calculations. The XPS core-level spectra revealed systematic shifts, for which the change of the Mo-Mo intercluster distances may be responsible. From the fact that the valence-band spectra do not agree with the rigid-band model, we propose that the narrowing of the Mo $4d$ bands caused by the insertion of Sn atoms explains the observed shift. An indication of the energy gap located ~ 1 eV above the Fermi level characteristic of the Chevrel system was obtained in the BIS spectra. We have also calculated the band structure of Mo_6Se_8 and $SnMo_6Se_8$ and compared them with the experiment. The overall good agreement between theory and experiment in a wide energy range shows that the LDA is valid for these compounds. On the other hand, the high DOS due to the VHS was reduced in the experimental spectra. While it has been reported several times that band-structure calculations well reproduce the experimental valence-band spectra,[12,13] this discrepancy was found in the present study because of higher energy resolution than in previous work.

Our results imply that the insertion of various atoms between the clusters influences the electronic structure around E_F through a change in the intercluster interaction, resulting in a change beyond the simple rigid-band picture. The flexibility of the insertion of cations into the unique cluster-based structure is attractive and, besides the possibility of application as thermoelectric materials, there may lie other aspects in the Chevrel-phase and related compounds such as one-dimensional compounds made of Chevrel clusters.[35] Systematic theoretical and experimental studies are needed to clarify the relationship between the inserted atoms and the electronic structures around E_F. Such information would be useful to finely tune the electronic properties of the Chevrel-phase compounds.

ACKNOWLEDGMENTS

The authors would like to thank T. Mizokawa, K. Mamiya, and T. Konishi for their technical support and informative discussions. K.K. was supported by the Japan Society for the Promotion of Science for Young Scientists.

*Present address: Institute for Solid State Physics, University of Tokyo, Kashiwa 277-8581, Japan.

†Present address: Indian Institute of Technology, Bombay Powai, Mumbai 400076, India.

[1] *Superconductivity in Ternary Compounds I*, edited by Ø. Fischer and M. B. Maple, Vol. 32 of *Topics in Current Physics* (Springer, Berlin, 1982).

[2] S. V. Vonsovsky, Y. A. Izymuov, and E. Z. Kurmaev, *Superconductivity of Transition Metals* (Springer, Berlin, 1982), pp. 418–431.

[3] Ø. Fischer, Appl. Phys. **16**, 1 (1978).

[4] C. Roche, R. Chevrel, A. Jenny, P. Pecheur, H. Scherrer, and S. Scherrer, Phys. Rev. B **60**, 16 442 (1999); C. Roche, P. Pecheur, G. Toussaint, A. Jenny, H. Scherrer, and S. Scherrer, J. Phys.: Condens. Matter **10**, L333 (1998).

[5] R.W. Nunes, I.I. Mazin, and D.J. Singh, Phys. Rev. B **59**, 7969 (1999).

[6] L.F. Mattheiss and C.Y. Fong, Phys. Rev. B **15**, 1760 (1977).

[7] D.W. Bullett, Phys. Rev. Lett. **39**, 664 (1977).

[8] O.K. Andersen, W. Klose, and H. Nohl, Phys. Rev. B **17**, 1209 (1978).

[9] T. Jarlborg and A.J. Freeman, Phys. Rev. Lett. **44**, 178 (1980).

[10] H. Nohl, W. Klose, and O. K. Andersen, in *Superconductivity in Ternary Compounds I* (Ref. 1), pp. 165–221.

[11] H. Ihara and K. Kimura, Jpn. J. Appl. Phys., Suppl. **17**, Suppl.17-2,281 (1978).

[12] E.Z. Kurmaev, Yu.M. Yarmoshenko, R. Nyholm, N. Mårtensson, and T. Jarlborg, Solid State Commun. **37**, 647 (1981).

[13] A. Fujimori, M. Sekita, and H. Wada, Phys. Rev. B **33**, 6652 (1986).

[14] F.C. Brown, B.A. Bunker, D.M. Ginsberg, T.J. Miller, W.M. Miller, and E.A. Stern, Phys. Rev. B **34**, 7698 (1986).

[15] S. Suga, K. Soda, T. Mori, M. Yamamoto, K. Kitazawa, and S. Tanaka, J. Phys. Soc. Jpn. **55**, 2102 (1986).

[16] S. Yashonath, M.S. Hegde, P.R. Sarode, C.N.R. Rao, A.M. Umarji, and G.V. Subba Rao, Solid State Commun. **37**, 325 (1981).

[17] H. Namatame, K. Soda, T. Mori, M. Fujisawa, M. Taniguchi, S. Suga, K. Kitazawa, and S. Tanaka, Jpn. J. Appl. Phys., Part 2 **28**, L266 (1989).

[18] R. Flükiger and R. Baillif, in *Superconductivity in Ternary Compounds I* (Ref. 1), pp. 114–141.

[19] H. Wada, M. Onoda, H. Nozaki, and I. Kawada, J. Less-Common Met. **113**, 53 (1985).

[20] S. Hüfner, *Photoelectron Spectroscopy* (Springer, Berlin, 1994); G. K. Wertheim and P. H. Citrin, in *Photoemission in Solids Vol. I*, edited by M. Cardona and L. Ley (Springer, Berlin, 1978).

[21] X. Li, Z. Zhang, and V.E. Henrich, J. Electron Spectrosc. Relat. Phenom. **63**, 253 (1993).

[22] J.-J. Yeh and I. Lindau, At. Data Nucl. Data Tables **32**, 1 (1985).

[23] O.K. Andersen, Phys. Rev. B **12**, 3060 (1975).

[24] O.K. Andersen and O. Jepsen, Phys. Rev. Lett. **53**, 2571 (1984).

[25] O. Jepsen and O.K. Andersen, Z. Phys. B: Condens. Matter **97**, 35 (1995).

[26] G. Krier, O. K. Andersen, and O. Jepsen (unpublished).

[27] W.R.L. Lambrecht and O.K. Andersen, Phys. Rev. B **34**, 2439 (1986).

[28] O. Jepsen and O.K. Andersen, Solid State Commun. **9**, 1763 (1971); P. Blöchl, O. Jepsen, and O.K. Andersen, Phys. Rev. B **49**, 16 223 (1994).

[29] T. Morikawa and T. Takahashi, Solid State Commun. **87**, 1017 (1993); L.H. Tjeng, R. Hesper, A.C.L. Heessels, A. Heeres, H.T. Jonkman, and G.A. Sawatzky, *ibid.* **103**, 31 (1997).

[30] F. Zwick, H. Berger, I. Vobornik, G. Margaritondo, L. Forró, C. Beeli, M. Onellion, G. Panaccione, A. Taleb-Ibrahimi, and M. Grioni, Phys. Rev. Lett. **81**, 1058 (1998).

[31] S. Engelsberg and J.R. Schrieffer, Phys. Rev. **131**, 993 (1963).

[32] O. Gunnarsson, H. Handschuh, P.S. Bechthold, B. Kessler, G. Ganteför, and W. Eberhardt, Phys. Rev. Lett. **74**, 1875 (1995); M. Knupfer, M. Merkel, M.S. Golden, J. Fink, O. Gunnarsson, and V.P. Antropov, Phys. Rev. B **47**, 13 944 (1993).

[33] I.H. Inoue, I. Hase, Y. Aiura, A. Fujimori, Y. Haruyama, T. Maruyama, and Y. Nishihara, Phys. Rev. Lett. **74**, 2539 (1995).

[34] K. Morikawa, T. Mizokawa, K. Kobayashi, A. Fujimori, H. Eisaki, S. Uchida, F. Iga, and Y. Nishihara, Phys. Rev. B **52**, 13 711 (1995).

[35] R. Brusetti, O. Laborde, A. Sulpice, R. Calemczuk, M. Potel, and P. Gougeon, Phys. Rev. B **52**, 4481 (1995).

[36] A. Fujimori, K. Kobayashi, T. Mizokawa, K. Mamiya, A. Sekiyama, H. Eisaki, H. Takagi, S. Uchida, R.J. Cava, J.J. Krajewski, and W.F. Peck, Jr., Phys. Rev. B **50**, 9660 (1994); K. Kobayashi, T. Mizokawa, K. Mamiya, A. Sekiyama, A. Fujimori, H. Takagi, H. Eisaki, S. Uchida, R.J. Cava, J.J. Krajewski, and W.F. Peck, Jr., *ibid.* **54**, 507 (1996).